Systems Design of MARIO: Stand-Alone 16U CubeSat from Earth to Mars

Mani, Karthik; Casado, AS; Franzese, V; Topputo, Francesco; Cervone, Angelo

Publication date
2019

Document Version
Final published version

Published in
IAF 70th International Astronautical Congress

Citation (APA)
Mani, K., Casado, AS., Franzese, V., Topputo, F., & Cervone, A. (2019). Systems Design of MARIO: Stand-Alone 16U CubeSat from Earth to Mars. In *IAF 70th International Astronautical Congress* (Vol. 2019-October). Article IAC{19{B4.8.3.x50968 (Proceedings of the International Astronautical Congress, IAC).

IAC–19–B4.8.3.x50968

Systems Design of MARIO: Stand-alone 16U CubeSat from Earth to Mars

Karthik Venkatesh Mani
Politecnico di Milano, Italy
karthikvenkatesh.mani@polimi.it

Alvaro Sanz Casado
Airbus Defence & Space, Spain
airbus.sanz-casado@airbus.com

Vittorio Franzese
Politecnico di Milano, Italy
vittorio.franzese@polimi.it

Francesco Topputo
Politecnico di Milano, Italy
francesco.topputo@polimi.it

Angelo Cervone
TU Delft, the Netherlands
a.cervone@tudelft.nl

Mars Atmospheric Radiation Imaging Orbiter (MARIO) is a 16U stand-alone CubeSat mission that shall escape Earth, perform autonomous deep-space cruise, achieve ballistic capture, and enter an operational orbit at Mars to perform thermal radiation imaging. This work focuses on the systems design of MARIO. The design of combined chemical-electric propulsion systems, comprising FLP-106 based green chemical monopropellant thruster and the iodine-fueled RF ion thruster, for hybrid high-thrust–low-thrust Earth–Mars transfer is presented. Reflectarrays along with high-gain antennas are utilised to establish long-distance low-bandwidth X-band communication link with the Earth. Electrical power system design is pursued to provide steady power to the system during the transfer and science operations phases. A novel autonomous navigation strategy is proposed which includes horizon-based optical navigation near target bodies and deep-space line-of-sight navigation for accurate state estimation for autonomous operations. Details regarding on-board processing, attitude determination, and thermal control are delineated. Feasible budgets for mass and communications link are obtained. The structural composition of MARIO is detailed.

1. Introduction

CubeSats have been extensively used for Low-Earth Orbit Missions with significant success. The multifarious applications include climate assessment, atmospheric characterization, biological research etc [1]. CubeSats are primarily developed by universities and small-spacecraft consortia owing to their ability to perform significant science observations at very low development costs. Contemporary CubeSats operate at Low-Earth Orbits (LEOs) and their size range is 1U to 6U while larger form factors are under development [2].

Interplanetary CubeSat missions expand the horizon of CubeSat applications and enable Solar System exploration at a high science-to-investment ratio [3]. They open up the access to deep space for institutions and companies that are smaller than the traditional large national and international space agencies and corporations, thereby leading to a democratization of space. This shall boost the satellite system development efforts and result in significant scientific and technological advances. Mission applications include Mars science observation, Mars communication relay and network setup [4], asteroid mineral mapping, heliophysics studies [3], lunar meteoroid observation [2] etc.

CubeSat missions to Mars could be achieved through a) in-situ deployment by a mother ship and b) highly flexible stand-alone Cubesats on deep-space cruise. The MarCO mission, designed by JPL and launched alongside InSight lander mission in May 2018, is the only interplanetary CubeSat in existence [5]. The mission is launched in the interplanetary space from the mother ship and performs a Mars flyby to provide communication support during InSight's landing. Stand-alone CubeSats to near-Earth objects are shown to be feasible, such as the Miniaturised Asteroid Remote Geophysical Observer (M-ARGO) mission study by the European Space Agency [6]. Improvements in critical fields like long-distance communication, deep-space autonomous guidance-navigation-control, propulsion for trajectory control, accurate ADCS, and high-speed low-power on-board data processing could push the envelope to 1.5 AU, thereby making a stand-alone Mars CubeSat feasible.

To this extent, a stand-alone CubeSat mission, the ***M**ars **A**tmospheric **R**adiation **I**maging **O**rbiter (MARIO)*, is envisaged. MARIO is a 16U stand-alone CubeSat exploration mission to Mars that

shall demonstrate the capabilities of CubeSats to escape Earth, perform autonomous deep-space cruise, achieve ballistic capture, and enter an operational science orbit at Mars. It shall utilise combined chemical-electric propulsion, concomitant with hybrid high-thrust–low-thrust trajectories and autnomonous guidance, navigation and control. The mission shall conduct thermal radiation imaging to characterize the thermal environment in the Mars upper atmosphere. It shall serve as a pioneer for standalone interplanetary missions with high launch flexibility and cost efficiency.

This work presents the phase zero systems design of MARIO. Section 2 delineates the mission characteristics of MARIO. Section 3 highlights the engineering objectives, top-level requirements and the system architecture. In section 4, the design of combined chemical–electric propulsion systems, electrical power system, communications system, autonomous navigation strategies as well as other subsystems such as on-board processing, attitude control and thermal control are detailed. Section 5 presents the structure and system configuration of MARIO, along with mass and volume budgets.

2. Mission Characteristics

The MARIO mission shall demonstrate the capabilities of CubeSats to perform a) orbit raising & Earth escape, b) heliocentric transfer c) ballistic capture at Mars and d) acquisition of the final operating orbit. These are the 4 key phases of this mission. The MARIO mission utilizes combined chemical–electric propulsion systems for executing a hybrid high-thrust–low-thrust trajectory.

The spacecraft is injected into a highly-eccentric Supersynchronous Geostationary Transfer Orbit (SSGTO) with a perigee of 295 km and an apogee of 90,000 km. Some contemporary geostationary satellite missions are launched into SSGTO and then utilize electric propulsion for apogee reduction and circularization to GEO; e.g. Falcon 9 v1.1 rocket launched Thaicom 6 in January 2014 into this orbit and Thaicom 8 in May 2017 into a 350 km × 90 226 km orbit*. Since the number of communication satellite launches (> 5 per year) are higher than that of direct deep-space launches ($\sim$1 per year), this orbit is selected to (a) improve the launch opportunities and widen the launch window, (b) reduce the ΔV required for Earth escape, and (c) provide more flexibility and autonomy to the CubeSat mission by diminishing its dependence on larger interplanetary spacecraft.

The presence of Van Allen radiation belts poses a significant risk of radiation damage to the spacecraft. Thus, a swift escape is necessary to avoid excessive damage. A high-thrust chemical propulsion system is used to provide a high ΔV within a short duration for orbit raising and Earth escape. A low-thrust electric propulsion system instead will drastically increase the residence time of the spacecraft in the radiation belts. The maneuvers are split and multiple orbit raisings are pursued to effectively distribute the ΔV and achieve Earth escape within a short timeframe while controlling gravity losses. Figure 1a illustrates the orbit raising and escape using chemical propulsion. The chemical and electric propulsion modules are *two separate systems in the same spacecraft*. Chemical propulsion module comprises a monopropellant thruster that utilizes an Ammoniun Dinitramide (ADN)-based FLP-106 propellant. The characteristics of the chemical propulsion module and the corresponding trajectory for Earth escape is expounded in Ref. [8].

Once Earth escape is achieved, the chemical propulsion is shut-off and the heliocentric transfer to Mars is executed using low-thrust high-specific impulse electric propulsion (Figure 1b). A high-specific impulse system aids in saving valuable system mass and the cruise lasts for $\sim$3.5–4.5 years, culminating with ballistic capture [7]. Two strategies for optimal heliocentric transfer are investigated: a) time-optimal continuous thrusting to minimize flight time and b) fuel-optimal bang-bang thrusting control to minimize propellant consumption. Depending on the mission priority, one of the two techniques can be used. As the Sun-spacecraft distance increases, the generated power decreases and consequently the available power to the thruster decreases. This impacts the specific impulse and thrust.

At the end of the cruise, the spacecraft experiences a *ballistic capture* (Figure 1c): the spacecraft is *captured* into a temporary stable orbit about Mars, only by the virtue of the natural attractions of Mars and the Sun [7]. The orbit acquired by the spacecraft after ballistic capture is highly irregular, and thus unusable for continuous observation missions. A high-thrust manoeuvre using chemical propulsion is performed to reduce the initial eccentricity and stabilize the orbit. The circularization to 60,000 km orbit is completed through low-thrust propulsion (Figure 1d). At this orbit, the planned thermal camera

*Space Launch Report - Falcon 9 `http://www.spacelaunchreport.com/falcon9ft.html` and `https://www.spacex.com/missions`. Last visited: 30-09-2019

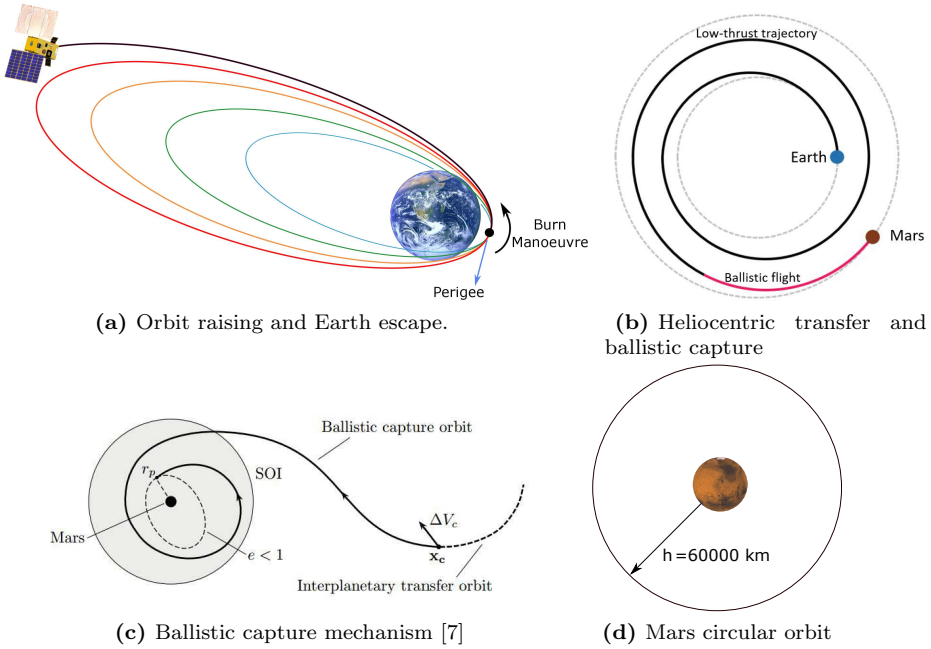

(a) Orbit raising and Earth escape.

(b) Heliocentric transfer and ballistic capture

(c) Ballistic capture mechanism [7]

(d) Mars circular orbit

Fig. 1: MARIO Mission Phases

payload will characterise the temperature in the Mars upper atmosphere.

3. Systems Engineering

3.1 Objectives and top-level requirements

The MARIO mission seeks to characterize the thermal environment of the Mars upper atmosphere using a camera that detects radiation in the visual and near-infrared ranges. The scientific mission of MARIO is fairly straightforward and open for further iteration. The primary challenge of MARIO is the technological demonstration of activities that have never before been achieved by CubeSats: escaping Earth, autonomous heliocentric transfer, achieving ballistic capture, and circularizing onto an operational orbit at Mars. The science objectives are achieved in conjunction with these. In the overall context, MARIO performs significant science at very low costs.

The major engineering objectives of MARIO are:

1. Demonstrate the feasibility of a stand-alone CubeSat to escape Earth, perform autonomous heliocentric transfer, achieve ballistic capture, and enter an operational orbit at Mars.
2. Demonstrate the feasibility of a CubeSat to establish communication with Earth from Mars orbit.
3. Demonstrate the usage of combined chemical–electric propulsion to achieve a stand-alone high-thrust–low-thrust Earth to Mars transfer.
4. Demonstrate the ability of a stand-alone CubeSat to withstand and operate effectively under high radiation conditions near Earth and in the interplanetary space.
5. Demonstrate the usage of optical navigation techniques for autonomous deep-space and near-planetary operations.

The major requirements of the MARIO spacecraft are listed in Table. 1.

3.2 Systems architecture

MARIO system physical and functional architecture is illustrated in Figure. 2. The systems present are the thermal imaging camera payload(P/L-CAM), chemical and electric propulsion (CPROP & EPROP), reflectarray communications system with high-gain and low-gain antennas (COMT-HGA & COMT-LGA), attitude determination and control systems (ADCS), a flexible electrical power system

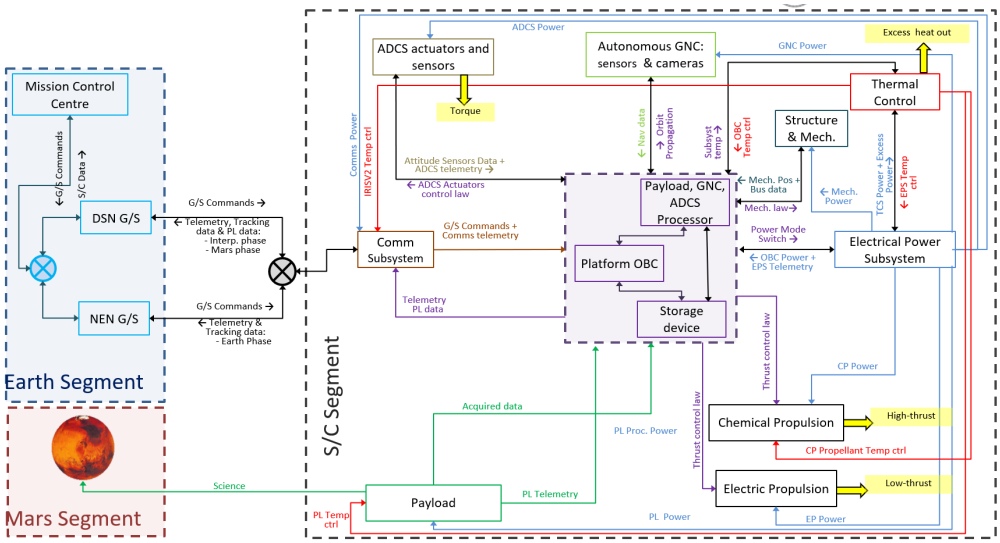

Fig. 2: MARIO system physical and functional architecture

Tab. 1: MARIO Overall System Requirements

ID	Requirement
OVRSYS-01	The mass of the spacecraft shall be no greater than 32 kg
OVRSYS-02	The spacecraft volume shall not exceed the configuration of a 16U CubeSat
OVRSYS-03	The system shall establish long-distance communication with Earth up to a range of 1.5 AU
OVRSYS-04	The system shall be operational for a minimum of 6 years

(EPS), a semi-active thermal control system (TCS), navigation camera (GNC CAM), a platform on-board computer (OBC), and a high speed processor for processing of payload data, ADCS data, and navigation data as well as on-board propagation of orbits for guidance.

4. Flight system design

4.1 Combined Chemical–Electric Propulsion

Chemical propulsion

MARIO uses a combined chemical–electric propulsion system for executing the Earth–Mars standalone tranfer. The two systems are separate and have *no resource sharing*. Chemical propulsion system comprises monopropellant thrusters utilizing FLP-106 propellant and the electric propulsion utilizes Iodine-fuelled inductively-coupled RF Ion thruster. Mani et al [8] have presented the detailed design strategies for the MARIO propulsion systems. The requirements for chemical (CP) and electric (EP) propulsion system are listed in Table. 2.

Tab. 2: Combined chemical–electric propulsion system requirements

ID	Requirement
PROP-01	The total mass of the combined chemical–electric propulsion systems shall be no more than 50% of the initial spacecraft mass.
CP-01	The CP system shall provide a minimum $\Delta V = 445$ m/s for orbital transfer and Mars orbit stabilization maneuvers.
CP-02	The CP system shall have a maximum thrust of 3 N
CP-03	The maximum thrusting time shall be 600 seconds per orbital manoeuvre
CP-04	The CP system shall utilize non-toxic propellants
EP-01	The maximum transfer time shall be 4.5 years for cruise and ballistic capture.
EP-02	The EP system shall have a maximum power consumption of 70 W

The maximum mass of the combined propulsion system is restricted to 50% of the total spacecraft mass. CP-01 is based on the ΔV requirement for Earth escape and Mars stabilization maneuvers. The

ΔV required for escape from the 295 km × 90 000 km injection orbit is 360 m/s, considering impulsive maneuvers at perigee. Considering real maneuvers, gravity losses and other miscellaneous operational errors, a 10% margin is added, thus $\Delta V_{esc,mg} = 396$ m/s. A deceleration manoeuvre to stabilize the orbit at Mars after ballistic capture requires $\Delta V_{stab} = 45$ m/s. With an additional ∼10% margin, $\Delta V_{stab,mg} = 49$ m/s. CP-03 and CP-04 establish the limitation on maximum thrust and burntime for a) effective distribution of ΔV to escape Earth into multiple maneuvers for transfer time reduction and gravity loss control, b) disturbance torque reduction and c) excessive heating avoidance. Non-toxic propellants need to be used (CP-04) since the MARIO is assumed to be a secondary payload and any damage to the primary payload as well as self-damage must be avoided.

Monopropellant thrusters that use green propellants have a good performance with regards to thrust and specific impulse [9]. They are relatively less complicated and are space qualified [10]. The propellant considered is a liquid blend of ADN - ammonium dinatramide ($NH_4[N(NO_2)_2]$), called FLP-106 with a liquid phase density of 1357 kg/m^3 at 25°C [11]. In comparison, the widely used monopropellant Hydrazine has a density of 1.004 kg/m^3 at room temperature and has a very high toxicity. FLP-106 has very low sensitivity and volatility. The I_{sp} yield of FLP-106 is also significantly higher than that of Hydrazine [12].

Thermochemical analysis of FLP-106 using the NASA Chemical Equilibrium Analysis (CEA) code is pursued to obtain the propellant performance [8]. Some key properties of FLP-106 and its performance are listed in Table 3.

Tab. 3: Properties of FLP-106

Property	**Value**
Molecular mass, $\mathfrak{M}$	22.8 kg/kmol
Liquid phase Density, ρ	1357 kg/m^3
Saturation temperature, T_s	273.15 K
Vapour pressure, P_{vap}	<21 mPa

The chemical thruster design is pursued with a target thrust of 3 N (CP-01). ADN-based thrusters providing 1 to 1.5 N thrust are currently under development [11]. To provide the necessary thrust, two 1.5 N thrusters can be utilized.

The chamber pressure is maintained at 2 MPa, which yields a similar thrust performance to the HPGP thruster on-board PRISMA satellite [10]. The CEA calculations yield ideal rocket performance parameters and the nozzle and combustion efficiencies need to be considered for real performance predictions. A conical nozzle with a throat diameter, D_t, of 0.75 mm is utilized. The average nozzle efficiency $\eta_n = 0.92$ and the combustion efficiency $\eta_c = 0.98$ are used [13]. A nozzle area ratio of $\varepsilon = 200$ is chosen for the design and the thruster performance parameters are listed in Table 4.

Tab. 4: Estimated thruster design and performance parameters

Property	**Value**
Throat diameter, D_t	0.75 mm
Expansion area ratio, ε	200
Chamber pressure, P_c	2 MPa
Chamber diameter, D_c	5.3 mm
Chamber volume, V_c	662.7 cm^3
Nozzle length, L_N	18.47 mm
Combustion efficiency, η_c	0.98
Nozzle efficiency, η_n	0.92
Max Thrust (per thruster)	1.536 N
Specific Impulse, I_{sp}	241.2 s
Characteristic velocity, c^*	1334.47 m/s
Thrust coefficient, C_F	1.7383
Mass flow rate (per thruster), $\dot{m}$	0.673 g/s
Chamber temperature, $\mathcal{T}_c$	2133.4 K

Spacecraft trajectory is calculated by assuming a 2-body problem, discarding perturbations, and integrating the equations of motion with the calculated thruster performance and the injection orbit as input. The overall ΔV imparted to the spacecraft and the overall propellant mass consumed are calculated. The thruster performance values of $T = 3$ N (CP-01) and $I_{sp} = 241.2$ s are utilized in this analysis. The burntime for each manoeuvre is calculated to be 598.6 seconds such that the overall flight time is kept to the minimum, i.e. 792.73 hours. This flight time is counted as the Earth orbiting time until eccentricity $e = 1$, and not the time to reach the Earth sphere of influence. The total number of maneuvers is 6 and the escape is achieved at the 7th orbit. The number of Van Allen belt crossings amount to 13. The orbital raising is illustrated in Figure 3.

The calculated cumulative ΔV_{esc} of the orbit raising and escape maneuvers is 363.14 m/s, which is ∼3 m/s higher than the ideal ΔV for escape. This difference corresponds to the accumulated gravity losses (ΔV_{gl} ∼1%). A 10% margin is placed on the ideal ΔV for contingency and $\Delta V_{esc,mg}$ is 396 m/s. The propellant mass ($m_{p,mg}$) pertaining to $\Delta V_{esc,mg}$ is 4.993 kg kg while the m_p for ΔV_{esc} is 4.553 kg. The stabi-

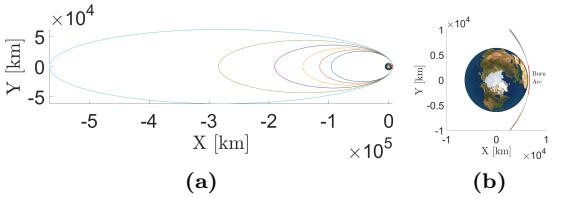

Fig. 3: MARIO orbit raising and escape - ballistic and burn trajectories

lization manoeuvre is executed after low-thrust heliocentric transfer and ballistic capture. The $\Delta V_{stab} = 45$ m/s and a 10% margin is again placed for contingency, thus making $\Delta V_{stab,mg} = 49$ m/s. The propellant mass $m_{p,stab} = 0.418$ kg and the margined value $m_{p,stab,mg} = 0.459$ kg. A 5% margin is placed on the propellant mass to account for the RCS thruster operations. Thus, the overall chemical propellant mass is 5.725 kg.

The feed system consists of the storage tanks, valves, flow lines, and the tank pressurization system. Considering the liquid phase density of FLP-106, 1357 kg/m^3, the total propellant volume is 4218.6 cm^3, which in terms of CubeSat units is ∼4.2U. A regulated pressure-fed system is utilized as the thrust must be precise and constant. Gaseous nitrogen GN_2 is used as the pressurant. Four cylindrical tanks with elliptical dome ends are utilized to accommodate them into the 16U CubeSat structure (see Figure. 14). A ∼10% ullage volume is applied and each tank occupies 1160.1 cm^3. Each tank has a diameter of 9.4 cm diameter and a height of 18.05 cm, thus occupying 1.8U.

The nominal feed pressure is set at 2.2 MPa and the Maximum Expected Operational Pressure (MEOP) is 2.6 MPa. The feed pressure value is similar to the one for a high-performance ADN-based monopropulsion system on-board PRISMA satellite [10]. A burst factor of 1.5 is applied on the MEOP to obtain the burst pressure. The pressurant gas (GN_2) pressure is considered to be 28 MPa at 323 K, at which the density is 257.8 kg/m^3 [14].

The material used for the tank is Titanium alloy Ti-6Al-4V, with a yield strength of 880 MPa and density of 4430 kg/m^3[15]. It has a very high corrosion resistance. The tank wall thickness is calculated for the burst pressure with a safety factor of 1.2 applied on the yield strength [16]. An additional safety factor of 2 is applied on the thickness considering launch loads and vibration. The major components of the monopropellant thruster system are illustrated in Figure 4. The feed system design characteristics are listed in Table 5.

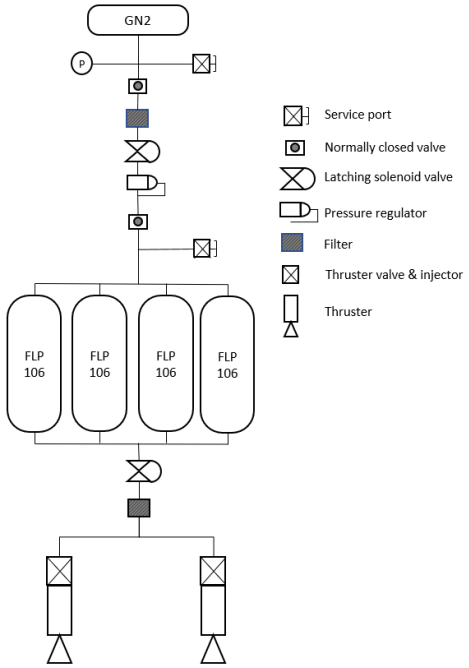

Fig. 4: Schematic of the monopropellant thruster system

Electric propulsion

Once Earth escape is achieved using the chemical propulsion system and the spacecraft reaches Earth's sphere of influence, the deep-space cruise phase starts. A high-I_{sp} electric propulsion system is utilized in this phase. The cruise lasts for ∼3.5–4.5 years and culminates in ballistic capture [7]. Transfer to Mars after Earth escape is achieved by thrusting continuously, thereby minimizing flight time.

Electric propulsion requirements are listed in Table. 2. EP-01 constrains the maximum transfer time to 4.5 years such that valuable science products can be obtained before the end of the mission lifetime, ∼6 years. Owing to the restricted power availability, EP-02 imposes a maximum limit on the power consumption of the thruster. Both thrust and I_{sp} vary with thruster power. The power available to the electric propulsion system is calculated as a function of the distance between the spacecraft and the Sun. Figure 5 illustrates the available and consumed power for the MARIO mission. The total power available at 1 AU at BOL is 202 W and at 1.5 AU at EOL is 85.75 W (see section 4.2). Critical subsystems such as communications, on-board computer, attitude control, and

Tab. 5: Monopropellant system design parameters

Parameter	Value
Initial Mass, m_0	30 kg
Propellant mass, $m_{p,esc}$ (ΔV_{esc})	4.553 kg
Propellant mass, $m_{p,esc,mg}$ ($\Delta V_{esc,mg}$)	4.993 kg
Propellant mass, $m_{p,stab}$ (ΔV_{stab})	0.418 kg
Propellant mass, $m_{p,stab,mg}$ ($\Delta V_{stab,mg}$)	0.459 kg
Propellant mass, $m_{p,rcs}$ (5% marg.)	0.273 kg
Propellant mass (total), $m_{p,mg,tot}$	5.735 kg
Propellant tanks	4
Prop. tank volume (each), V_{tank}	1160.1 cm^3
Prop. tank diameter, $d_{prop,tank}$	9.4 cm
Prop. tank height, $h_{prop,tank}$	18.05 cm
Prop. tank burst pressure, $P_{prop,burst}$	3.9 MPa
Prop. tank thickness, $th_{prop,tank}$	0.50 mm
Prop. tank mass (total), m_{tank}	0.219 kg
Press. gas mass, m_{gas}	0.127 kg
Press. tank volume, $V_{gas,tank}$	492 cm^3
Press. tank diameter, $d_{gas,tank}$	9.4 cm
Press. tank height, $h_{gas,tank}$	7.76 cm
Press. tank thickness, $th_{gas,tank}$	4.5 mm
Press. tank mass, $m_{gas,tank}$	0.238 kg
Feed pipes & valves mass, m_{fv}	0.20 kg
Thrusters mass, $m_{thrusters}$	0.4 kg
Feed system total volume	8U
Overall chemical propulsion mass, $m_{cp,sys}$	6.91 kg
Overall volume, $V_{cp,sys}$	8U

electrical power system operate continuously during the transfer. The combined power consumption of these subsystems is ∼40 W. Cell degradation, neutralization losses and the power processing and control unit (PPCU) consumption (3 W) are included in the thruster input power calculations. The minimum power supplied to the thruster (at ∼1.5 AU) is 37.9 W.

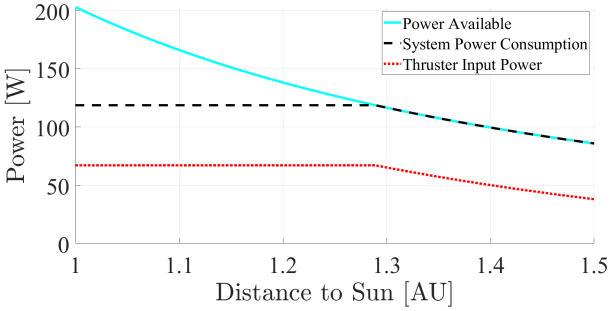

Fig. 5: Available and consumed powers variation with Sun-spacecraft distance for MARIO mission

The type of electric propulsion system chosen for MARIO is a miniature inductively coupled radiofrequency gridded ion thruster. They have a high lifetime and a high performance for the given input power range [8]. Additionally, gridded ion thrusters are compatible with multiple propellants such as xenon, argon, krypton and iodine. Electromagnetic interference of ion thrusters is also much lower compared to Hall thrusters.

Iodine (I_2 or I) is used as the propellant and has a molecular mass of 126.9 kg/kmol (monoatomic). It is a solid in standard atmospheric conditions with a density of 4940 kg/m^3. This eliminates the need for high pressure tanks, complicated plumbing, and sophisticated thermal control systems, which are otherwise required in the case of xenon. Iodine stored in a solid state in compact lightweight tanks can be moderately heated to sublimate and form I_2 vapour. A stand-alone CubeSat on a deep-space cruise to reach Mars requires a high ΔV and subsequently a large propellant mass. Compactness of iodine makes it highly suitable for such CubeSat missions since the propellant can be easily accommodated within the structure. Additionally, the cost of pure iodine is ∼$400 per kg, which is very cheap compared to xenon.

A performance model of an Iodine-fueled inductively coupled miniature radiofrequency gridded ion thruster is implemented and the performance parameters such as thrust, specific impulse, beam current and efficiencies are determined [8]. For the performance model, the chosen design and operational parameters are listed in Table 6. The thruster size is similar to that of the BIT-3 thruster [17]. A total mass flow rate of 48μg/s is chosen and the mass flow to the neutralizer cathode is fixed at 10%. The DC grid voltage V_{grid} is set at 2000 V.

Tab. 6: RF thruster performance model parameters

Parameter	Value
Thruster radius, R	1.25 cm
Thruster length, L	2.2 cm
Mass flow rate, $\dot{m}_0$	48 μg/s
Chamber volume, V	10.792 cm^3
Grid voltage, V_{grid}	2000 V

The variations of thrust, I_{sp} and η with power are illustrated in Figure 6. The thruster performance values are listed in Table 7.

Earth–Mars transfer trajectory optimization is performed to target a defined ballistic capture point at a set epoch. As the Sun-spacecraft distance increases, the available power decreases and the thruster performance is affected. The spacecraft de-

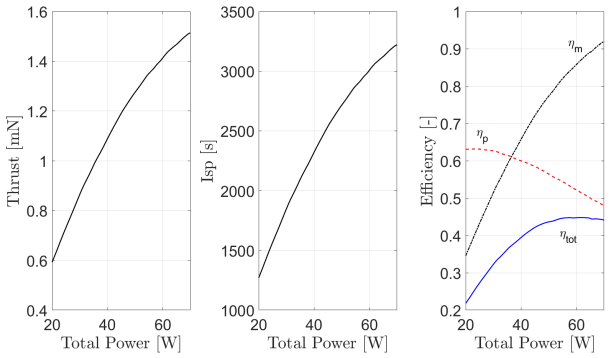

Fig. 6: Thrust, I_{sp} and efficiencies vs total power

Tab. 7: RF thruster performance at maximum power (67 W)

Parameter	Value
Max Thrust, T_{max}	1.492 mN
Max I_{sp}	3168 s
Max Beam Current, I_{beam}	16.5 mA
Power efficiency, η_p	49.2%
Mass utilization efficiency, η_m	90.33%
Total efficiency, η_{tot}	44.44%

parts from a distance of 0.01 AU from Earth (Hill sphere radius), outward on the Sun–Earth line. An optimal control problem is solved to minimize the flight time (time-optimal). The mass of the spacecraft after high-thrust Earth escape is 27.02 kg. The transfer trajectory, the variation of heliocentric eccentricity and semi-major axis, and the thruster performance are illustrated in Figure 7. The time-optimal solution yields a total transfer time of 1250 days ($\sim$ 3.28 years), which satisfies EP-01, and the thruster operation time is 1186.83 days (3.42 years). The spacecraft is then circularized onto a 60000 km circular orbit using Q-law thrusting control [18]. Circularization takes 192.64 days and consumed 0.215 kg propellant.

The time-optimal heliocentric transfer and circularization require an overall propellant mass of 5.11 kg. A $\sim$10% margin is applied on this mass for contingency and an extra 5% for station-keeping at Mars, which brings it to 5.87 kg. Iodine solid state density is 4940 kg/m^3 and corresponding propellant volume is $\sim$1190cm^3. The propellant tank is sized to contain solid Iodine and the low-power heat source. The latter occupies 5% of the volume. Additionally, a 5% ullage volume is allocated for the sublimated gas,

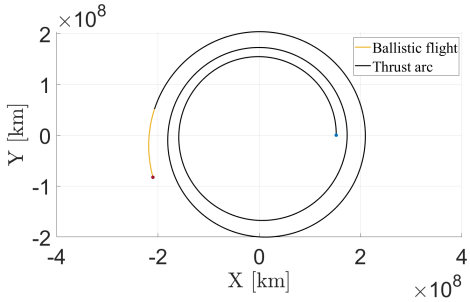

(a) Time-optimal trajectory

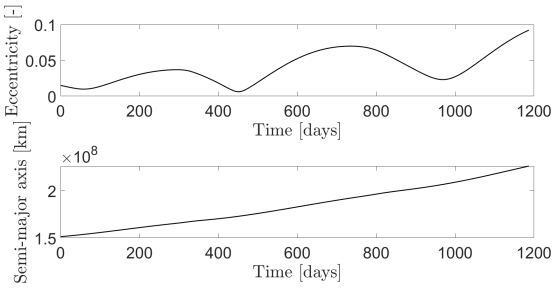

(b) Time-optimal heliocentric e and a

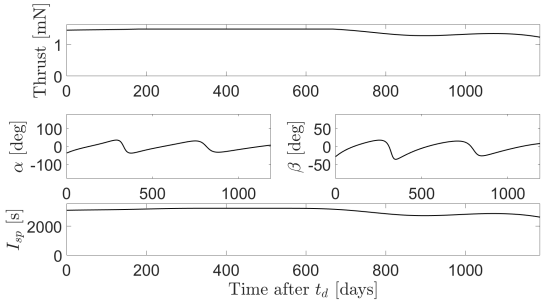

(c) Thrust & I_{sp}

Fig. 7: Spacecraft heliocentric trajectory, eccentricity e and semi-major axis a, and thruster performance variation in time-optimal transfer.

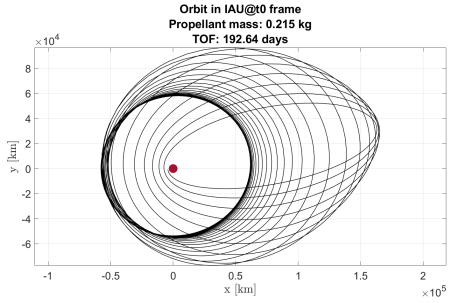

Fig. 8: Circularization onto 60000 km orbit about mars

bringing the total to 1308 cm^3. The electric propulsion system schematic is illustrated in Figure 9.

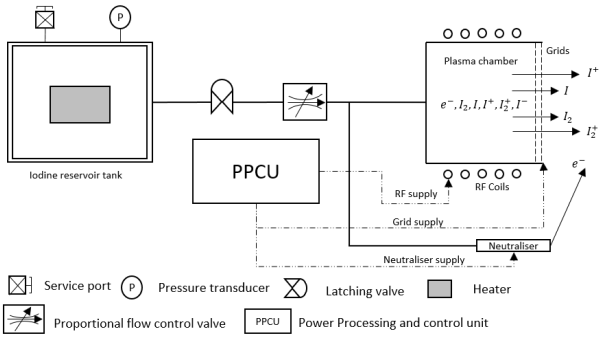

Fig. 9: Schematic of the electric propulsion system

Tab. 8: Electric propulsion design parameters

Parameter	Value
Propellant mass, $m_{p,mg}$	5.87 kg
Feed sys. mass, m_{feed}	0.5 kg
PPCU Mass, m_{PPCU}	0.2 kg
Thruster mass, m_T	0.2 kg
Tank volume	1308 cm^3
EP total mass, $m_{ep,sys}$	6.57 kg

4.2 Power

Steady power generation is ensured using two solar arrays connected to SADA mechanisms for continuous Sun pointing. Table 9 contains EPS requirements. The solar array sizing is determined by the the power required by the electric propulsion during the heliocentric transfer as well as the power demand while communicating from Mars orbit. Table 10 details the power consumption of individual subsystems and Table 11 shows the power consumption during different operational modes of the mission. MARIO systems consume 101 W (111 W with 10% margin) while it is in "full" low-thrust manoeuvre (LTM) mode. This mode is active in the interplanetary phase. However, the power generation varies with the Sun-spacecraft distance by the inverse square law. Since the required size of solar arrays for delivering 111 W for the different subsystems throughout the mission (taking into account generation and distribution losses) would be enormous, and since the science operations do not require such high power supply, a trade-off is performed and a compromise solution is taken: the power subsystem shall deliver 80W at Mars distance.

Tab. 9: Power system requirements

ID	Requirement
EPS-01	The system shall have Sun pointing capabilities.
EPS-02	The system shall provide at least 80 W to MARIO subsystems at 1.5 AU distance from the Sun after heliocentric transfer.
EPS-03	The battery shall provide at least 31 W for spacecraft survival in eclipse mode.
EPS-04	The EPS shall be able to dissipate the excess power generated to avoid spacecraft overheating

Tab. 10: MARIO subsystems power consumption

Subsystem	Nominal Power [W]	Remarks
P/L-CAM	7,0	
P/L-PROC	10,0	Also used in AOCS
EPS	1,0	Supply and distribution
COMT HGA	41,2	Transmit and Receive 10 W feeding
COMT LGA	33,2	Transmit and Receive 2 W feeding
COMR	12,6	Only Receive
OBC	0,8	Main Computer and Data Handler
AOCS	16,1	RW, STR, Sun sensor, IMU, PLCPROC/2
EPROP	70,0	Could be reduced affecting performance
CPROP	14,0	
TCS	10,0	Could be addapted
MECH	2,0	Deployment and Solar Array orientation
GNC CAM	0,7	

Tab. 11: MARIO power operational modes

Mode	Acronym	Peak Power [W] w/ 10% margin	Active systems
Commissioning	CMS	70	EPS, OBC, AOCS, COMT-LGA, MECH
Chem Man. Mode	HTM	49	EPS, OBC, AOCS, CPROP, MECH
Cruise Mode	CRU	34	EPS, OBC, AOCS, MECH, GNC-CAM, TCS
Near Earth Comm Mode	NEC	70	EPS, OBC, AOCS, COMT-LGA, MECH, TCS
Elec Manoeuvre Mode	LTM	111	EPS, OBC, AOCS, EPROP, MECH, GNC-CAM, TCS
Deep-space Comm Mode	DSC	79	EPS, OBC, AOCS, COMT-HGA, MECH, GNC-CAM, TCS
Science Mode	SCM	46	EPS, OBC, AOCS, PL-CAM, PL-PROC, MECH, TCS
Safe Mode	SFM	45	EPS, OBC, AOCS, COMR, TCS
OptNav Mode	NAV	37	EPS, OBC, AOCS, PL-CAM (Nav-mode), MECH, TCS
Eclipse Mode	ECL	31	EPS, OBC, AOCS, TCS

Figure 15 depicts MARIO solar arrays. Each one consists of 4 panels (22x45 cm) with 25 solar cells. The selected solar cells are the Azurspace 3G30C 30% efficiency cells. This means a total cell area of 0.6 m^2. Assuming a 10% inherent degradation and a 0.9% yearly degradation, the power generation capability will be 220 W BOL at Earth distance and 95 W EOL at Mars distance after 6 years. Taking into account an average 92% power distribution efficiency and 5 deg cosine losses, the power available to the subsystems will be 202 W at 1 AU at BOL and 85.75W at 1.5AU at EOL.

Figure 10 represents a schema of the electrical interfaces of MARIO CubeSat. Two Gomspace Nanopower BPX 77W/h batteries will be used as secondary power source to cover eclipse phases and peaks demand (see Figure 14). Besides, the Gomspace Nanopower P60 serves as PMAD (Power Management And Distribution) unit and equips two PDU (Power Distribution Unit) and two ACU (Array Conditioning Unit). This PMAD units will enable a flexible electrical power system architecture to enhance power management. On the one hand, each ACU is connected with several lines to a solar array. On the other hand, the PDUs distribute the power among the different subsystems using suitable lines.

4.3 Communications

Table 12 lists communications subsystem requirements. Establishing a direct communication link from MARIO to Earth at more than 1 AU distance is one of the most important challenges of this mission. CubeSats cannot equip conventional parabolic reflectors as larger interplanetary spacecraft do and the power available is much more limited. These facts compels us to pursue an innovative solution for interplanetary CubeSat communications. The deep-space communications strategy for MARIO is based on a deployable reflectarray high gain antenna (HGA) combined with IRIS transponder. MarCO mission used this technology serving as a data relay for Insight lander [19] successfully. Furthermore, in 2018, ISARA mission transmitted to Earth with a reflectarray from LEO and M-ARGO ESA CubeSat is designed to employ this antenna for interplanetary communications. MARIO communications subsystem is completed with a low gain patch antenna (S-Band) that will be utilized to establish first contact with the Earth after launch and during the Earth orbit raising manoeuvre.

The deployable reflectarray is designed to fit on the 16U CubeSat configuration so it consists of three 20x44 cm panels. During the launch phase, the three panels are folded down forming a one single panel configuration. Later, the stack panel is deployed and then unfolded. Finally, the reflectarray feeder is also deployed, ending in a configuration that can be observed in Figure 15.

Tab. 12: Communications system requirements

ID	Requirement
COM-01	The system shall provide direct link to Earth to transmit telemetry.
COM-02	The system shall communicate with G/S using X-Band in Mars phase and in interplanetary phase.
COM-03	The system shall communicate with G/S using S-Band in Earth orbit.
COM-04	The system shall be able to transmit 3 kbps data rate from 1.5AU by means of a direct link to the Earth.
COM-05	The system shall BER shall be below 10^{-4}.
COM-06	The stack size of the HGA shall be below 45x23x4 cm.

The HGA antenna will operate in the X-Band frequency (8.4GHz) and will transmit data to the DSN. The estimated maximum gain for this antenna is about 29.95 dB taking into account a 42% efficiency. The power provided to the feeder is set to 10 W but it could be increased if there is enough power available to improve transmission performance. On the other side of the link, a 70 m DSN antenna will receive the data from MARIO.

The path losses are the main source of losses because of the huge distance that waves have to travel. From 1.5AU and with the selected frequency, the free space losses are 278 dB. On top of that, 1 dB loss is added to account for rain and atmospheric gases attenuation. Besides, the system noise temperature, which is the other main contributor to the attenuation of the signal is estimated at 140 K. Finally, average values for antenna pointing, polarization and modulation losses are taken. The required energy per bit noise ratio is set to 4 dB and the selected modulation is BPSK. According to Larson et al [20], the obtained BER will be below 10^{-4}. Under the described conditions, MARIO is able to transmit 3 kbps from 1.5AU distance. Table 13 summarizes the main parameters involved in the link computation and the achieved performances.

Since the distance from Earth to MARIO will vary along the mission, the maximum data rate that can

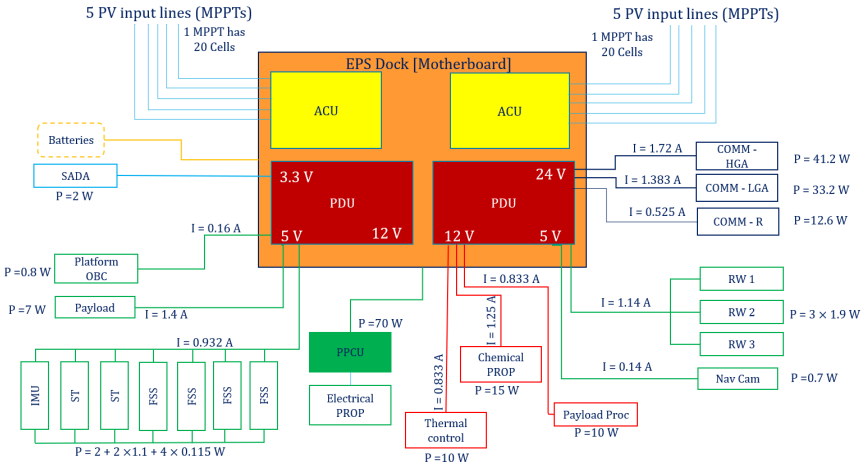

Fig. 10: MARIO electrical interface

Tab. 13: HGA link budget from 1.5AU

DOWNLINK BUDGET		
Assumptions		
DSN 70 m station	-	-
Madrid Avg. Rain	-	-
1 AU = 1,5·108 km	-	-
Distance = 1,3 AU	1,50	AU
Data Rate	3000	bps
Frequency		
Frequency	8420	MHz
Tx Antenna		
Feed power	10	W
Gain	30,0	dBi
Pointing Loss (1° pointing error)	-1,9	dB
Rx Antenna		
Gain	74,8	dBi
Pointing Loss	-0,1	dB
Losses		
Polarization Loss	-0,2	dB
Total Path Loss	-279,0	dB
System Noise Temperature	140,0	K
Transmitter Feeder Loss	-1,0	dB
Performance Parameters		
Equivalent Isotropic Radiated Power (EIRP)	39,0	dBm
Gain to Noise Temperature Ratio (G/T)	53,4	dB/K
Carrier to Noise Spectral Density Ratio (C/N0)	39,3	dBHz
Energy per Bit to Noise Ratio (Eb/N0)	4,1	dB
Modulation	BPSK + R-1/2 Vitervi	
(Eb/N0)req	4,0	dB
Recovery Margin	0,1	dB

be transmitted will also vary. Figure 11 illustrates the maximum data rate that could be transmitted as a function of MARIO–Earth distance and feeder input power taking into account the above-mentioned considerations for the link budget. The maximum data rate decreases significantly from 0.5 AU to 1.5 AU. Therefore, during Earth-Mars conjunction (0.5 AU distance), MARIO will be able to transmit about 25 kbps for 10 W feeder power. Nevertheless, the distance from the Earth to Mars increases up to 2.5 AU (planets opposition) which reduces dramatically the maximum data rate. In such case, MARIO can use its low gain antenna to transmit information to a larger Mars orbiter spacecraft which then would relay it to the Earth.

IRIS v2 transponder currently works with X-band and UHF bands. It is planned to extend its capabilities to other frequency bands like the S-Band. The transponder weights 1.2 kg and its nominal power consumption for X-band transmit/receive is 35 W for 3.8 W feeder power. Finally, ISM S-Band antenna manufactured by Endurosat is selected as the low gain patch antenna because of its low mass and performance.

4.4 Autonomous Navigation

The costs to navigate and operate CubeSats are still huge with respect to the other mission costs which scale down with the platform size. This is because the same ground tracking facilities and flight dynamics teams for large satellites are required. Thus, deep-space CubeSats like MARIO require high autonomy in GNC. In this framework, a novel autonomous navigation strategy is proposed which includes full-disk optical navigation near target bodies and celestial triangulation during deep-space cruise for autonomous state estimation. In object-proximity, horizon-based navigation methods exploit images of a nearly spherical object to estimate the current spacecraft position [21]. The goal is to estimate a camera-to-object relative position vector from

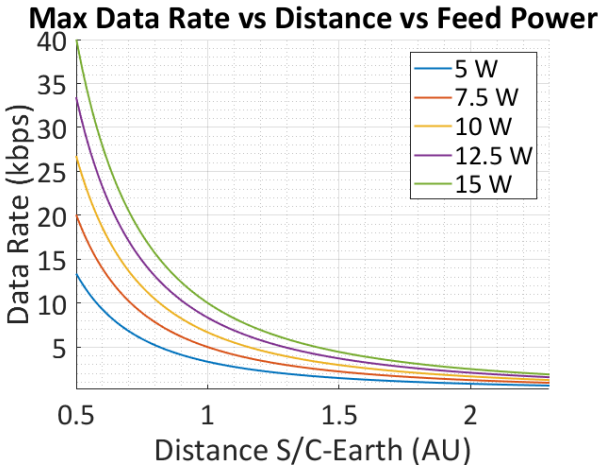

Fig. 11: Maximum data rate transmission as a function of distance and feed input power

the line-of-sight directions to some object full-disk points. The object full disk is estimated by fitting an ellipse to the observed lit horizon points, which are retrieved from 2D images (Figure. 12). The appli-

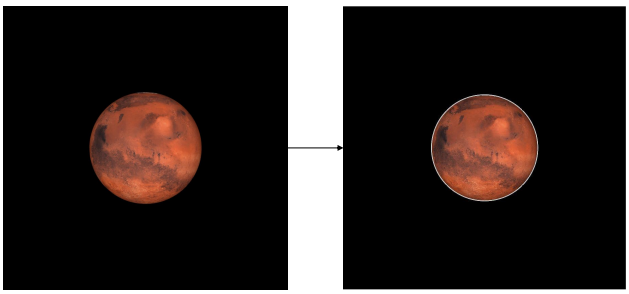

Fig. 12: Image Processing for horizon-based navigation.

cation of the horizon-based optical navigation to the MARIO mission case leads to a position accuracy as output of the image processing in the order of 100 km for the three position components (Figure 13). In deep-space, autonomous optical navigation relies on the estimation of a spacecraft state through the processing of the line-of-sight (LOS) directions to a number of visible targets. The visibility of these beacons is dictated by the observer-target geometry, the observer camera properties, and the beacon apparent magnitude. The LOS directions to the visible beacons can be extracted by the on-board camera to feed different LOS-based methods to estimate the probe state. The final expected 3σ accuracy in po-

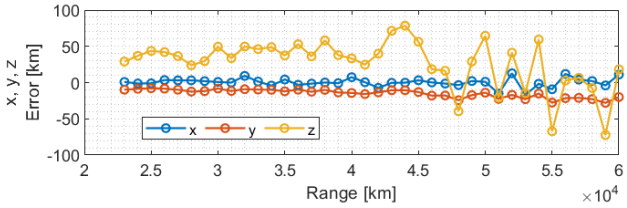

Fig. 13: Accuracy of horizon-based navigation.

sition determination is in the order of 1000 km for a typical CubeSat mission in deep-space [22].

4.5 Other subsystems

Semi-active thermal control system is designed to preserve the payload, propellants, and other subsystems within their operational temperature limits at near-Earth and interplanetary environments. This task will be performed by means of heaters, MLI and different surface finishes. To cool down the payload, the possibility of adding a dedicated radiator is considered.

Attitude determination and control will be carried out by the combination of several COTS. Two ST400 star trackers are installed in MARIO. They only consume 0.7 W in nominal operation and they have competitive attitude determination accuracy: 10 arseconds in pitch and yaw and 120 arcseconds in roll (3σ). To compensate the lower of accuracy in roll axis, the two STR are oriented along different axis. Both of them are equipped with baffles to reduce straylight and protect them against thursters' plume impingement. The update rate of ST400 STR is 5Hz, which is compatible with IMU performance. In addition, four fine sun sensors (nanoSSOC-D60) pointing towards different directions serve as a backup for attitude determination. These sun sensors have a 60 deg FOV and an accuracy of 0.5 deg. Finally, STIM300 IMU measures angular acceleration and velocity with 2000 SPS and with a 0.3 deg/h gyro bias instability. In the actuators side, 3 RW400 reaction wheels are responsible for the attitude control. Owing to their 50 mNms momentum storage capacity and their relatively low power consumption (1.9 W), RW400 are suitable for MARIO. Finally, four small 0.1 kg cold gas thrusters for reaction wheels desaturation and course correction complete the ADCS.

Skylab NanoOBC is the main On-Board computer. It is a light (about 60g) and robust device against SEE. The main OBC is in charge of general housekeeping and command transmission in MARIO. On

the contrary, the dedicated and more powerful payload processor deals with science data processing, attitude determination and orbit control and is also responsible for processing navigation information. The selected COTS is the Unibap e20xx. Despite it high power consumption, the performance is quite high.

The payload system consists on a customized VIS and IR camera and the above-mentioned payload processor. The maximum available weight for the payload camera to comply with spacecraft total mass requirements is about 1.8 kg and the maximum power consumption shall be below 7 W. The PL camera shall occupy less than 1.2U inside the CubeSat. The overall system characteristics are listed in Table 14.

Tab. 14: Overall system characteristics

Subsystems and Payload summary	
Propulsion	Chemical Propulsion: - 2 1,5N range thrusters - FLP-106 Propellant - High thrust maneuvers - Gaseous Nitrogean pressurant
	Electric Propulsion: - Gridded Ion Thruster - Iodine solid propellant - Low thrust trajectory and ballistic capture
Power	- 2 Deployable solar arrays with SADA - 30% Eff. Azurspace 3G30C solar cells - 2 GOMSpace BPX 77W/h batteries - PMAD: GOMSpace P60
Communications	- IRIS V2 Transponer - Reflectarray HGA X-Band - LGA S-Band
ADCS	- 3 RW: RW400 50mNms Hyperion Tech. - IMU STIM300 - 2 STR: ST400 Hyperion Tech. - 4 Sun Sensors: nanoSSOC-D60 Solar MEMS - 4 ADCS Cold gas thrusters
Data Handling	- Main OBC: NanoOBC Skylab
Structure	- 16U COTS modification - Aluminum shielding
Thermal Control	- 10W heaters power - MLI and coatings
Navigation	- NAV Camera: IM200 Hyperion Tech.
Payload	Payload Camera: - Customized VIS and IR Camera - 7W consumption and 1,8kg
	Payload Processor: - UNIBAP's e20xx/e21xx - Performs AOCS tasks too

5. Structure and System configuration

MARIO is a 16U CubeSat whose primary structure consists on 4 "decks" of 4U each. A 16U COTS structure doesn't exist at the moment (12U is the maximum) but several manufacturers could provide customized structures. The structure has to allow visibility access to the cameras and sensors as well as room for internal harnesses and feed system pipings of the thrusters. In addition to the structure, the different sides or panels have to be covered by an aluminum shielding layer to protect the spacecraft against radiation. Hereinafter, the sides of the CubeSat are referred as the PL panel (where is the PL camera), the Anti-PL panel (the opposite side), the bottom panel, the top panel, the right panel and the left panel.

The main drivers for the configuration are:

- Accommodation of 2 different types of propulsion.
- Power generation strategy.
- Having a unobstructed side for the PL camera.
- Communications with reflectarray.

The CP and the EP modules are placed on opposite sides of the CubeSat. The primary reason is that there is not enough space to hold both on one side. Besides, the center of mass with them placed on opposite sides is kept closer to the geometrical center of the spacecraft. Hence, the CP module is placed close to the the bottom panel, with the 2 CP thursters outside the structure, while the EP module is placed close to the top panel, with the ion engines outside (see Figure 14 and Figure 16). On the one hand, the four CP propellant tanks are located just above the bottom panel. The tanks itself occupy about 1.8U. The pressurizer tank position takes advantage of the shape of the CP propellant tanks and is installed in the central axis of the CubeSat. Therefore, above each CP propellant tank up to the upper half of the CubeSat there is 0.2U available space for piping. On the other hand, the iodine tank is placed centered on the top part of the structure. The PPCU is located close to it facing the PL panel.

The Solar Drive Actuators mechanisms (SADA) divide the CubeSat in two halves. The rotation axis of SADA is orthogonal to the right and left panels. The majority of the components of MARIO are located on the third deck of the structure. The PL is placed along the PL panel for Mars centre pointing and the PL processor is below it. The 3 RW are

oriented in 3 different axis and the IMU and 1 sun sensor are just above one of them. The Iris transponder and the OBC are stacked behind the PL so they are hidden in Figure 14. Finally, one STR, a navigation camera and the PMAD can be found in the remaining 1U space.

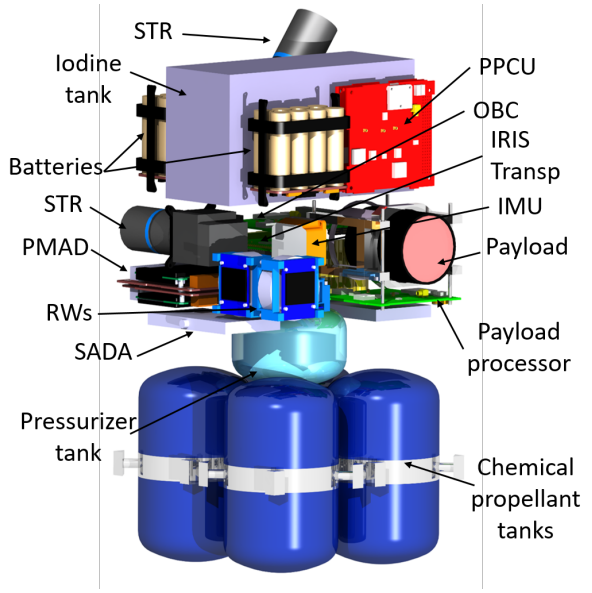

Fig. 14: MARIO internal configuration

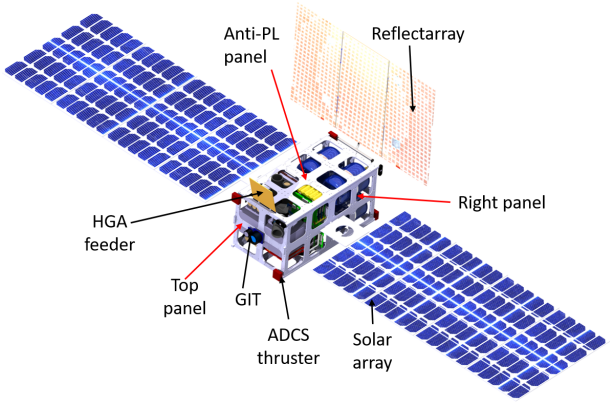

Fig. 15: MARIO external configuration w/o shielding

On the upper deck, apart from the EP module, batteries are symmetrically located with respect to the EP tank. In addition, another STR is placed tilted with respect to the orthogonal direction of the top panel. They are tilted because, primarily from the performance point of view, it is worse to have the STR along the same axis. That is the reason why the PL panel was discarded as a location. Besides, if the STR is oriented towards the right panel, it would be obstructed by the solar array eliminating that direction as an option. The direction orthogonal to the top panel would be suitable from performance point of view but not for potential plume impingement, which is the second driver. To reduce the plume impingement, the STR is tilted and a baffle is used to protect it.

In the outer part of the spacecraft, the rest of sun sensors (one on the top panel and two on the bottom panel) are installed. Besides, the 4 ADCS thrusters are placed symmetrically in the top and bottom panels. Reflectarray and its deployment mechanism are located on the outer side of the Anti-PL panel. Therefore, the feeder is also located in that panel. Finally, each solar array is attached to their corresponding SADA mechanism on the left and right panels. In stack configuration, both solar panels and reflectarray will be folded. The same applies to the feeder of the HGA antenna. Therefore, the outer envelope of the whole CubeSat will be 25x25x50cm.

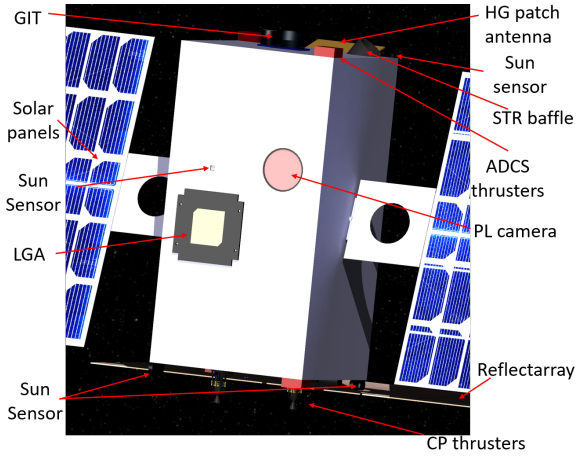

Fig. 16: MARIO external configuration Detail

5.1 Mass Budget

Table 15 shows the mass budget of MARIO CubeSat grouping components by subsystems. Figure 17 is a pie chart that represents the distribution of dry mass among subsystems. The table includes the subsystem level margin that depends on the design maturity of each subsystem/component (5, 10 or 20%) and the dry mass system margin which is set to 5%. On top of that, chemical propellant, pressurizer and iodine masses are added, obtaining the total wet mass.

Propellant and pressurizer masses already include a margin through the ΔV.

Tab. 15: Mass Budget of MARIO including unit and system margins

Item	Mass [kg]	Margin	Mass w/ margin [kg]	Design approach
Structure	4,326	5%	4,542	COTS with modification
EPS	3,964	5%	4,180	COTS with modification
Communications	1,982	5%	2,081	COTS with modification
ADCS	1,971	5%	2,070	COTS
ADCS Thursters	0,400	10%	0,440	COTS with modification
Navigation CAM	0,060	5%	0,063	COTS
Chemical Propulsion	1,06		1,223	
Propellant Tank	0,219	10%	0,241	Customized design
Thruster	0,400	20%	0,480	COTS
Feeding system	0,200	20%	0,240	Customized design
Press Tank	0,238	10%	0,262	Customized design
Electric Propulsion	0,70		0,810	
Propellant Tank	0,100	10%	0,110	Customized design
Thruster	0,200	20%	0,240	COTS
PPCU	0,200	10%	0,220	COTS with modification
Feeding system	0,200	20%	0,240	Customized design
Mechanisms	0,650	10%	0,715	COTS
OBC	0,058	5%	0,061	COTS
Harness	0,200	20%	0,240	COTS with modification
TCS	0,300	20%	0,360	COTS with modification
PL Camera	1,840	20%	2,208	Customized design
PL Processor	0,300	5%	0,315	COTS
Total Dry Mass	17,808		**19,31**	
System margin		5%		
Dry mass w/ marg.			**20,27**	
Chemical Propellant			5,72	Margin in Delta V
Pressurizer			0,13	Margin in Delta V
Iodine			5,87	Margin in Delta V
Total Wet Mass			**32,00**	

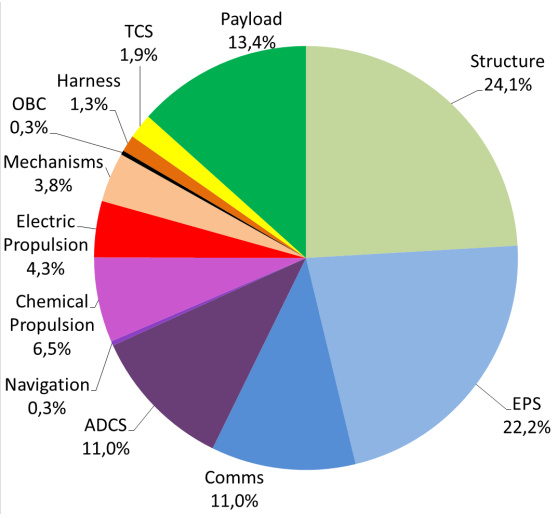

Fig. 17: Relative contribution of different subsystems to MARIO CubeSat

6. Conclusion

The Mars Atmospheric Radiation Imaging Orbiter (MARIO) is a 32 kg stand-alone 16U CubeSat exploration mission to Mars. It shall demonstrate the capabilities of a CubeSat to escape Earth, performa autonomous deep-space cruise, achieve ballistic capture, and acquire an operational orbit at Mars. It uses a novel combined chemical–electric propulsion system to execute a stand-alone Earth–Mars transfer on hybrid high-thrust–low-thrust trajectory, concomitant with autonomous guidance, navigation and control.

In this work, the mission characteristics of MARIO are highlighted and a systems design is performed to enable the mission. Details regarding the design of chemical propulsion system utilizing green monopropellant thrusters and electric propulsion systems utilizing iodine-fueled RF ion thrusters are presented. The overall mass of the combined chemical–electric propulsion system is 13.48 kg, which is ∼42% of the initial mass.

The electrical power system is designed to provide sufficient power the MARIO spacecraft during its interplanetary transfer phase as well as science & communication phase while at Mars orbit. The communications system utilises reflectarrays with a high-gain antenna and an IRIS V2 responder for long distance communication and a low-gain patch antenna for near-Earth communications. The communication link budget establishes a datarate of 3 kbps from 1.5 AU distance. Autonomous navigation strategies such as near-planetary horizon based navigation and deep-space line-of-sight navigation are highlighted. Details regarding other subsystems such as ADCS, on-board processing, and semi-active thermal control are also presented. Feasible budgets for communication and mass are presented along with a compact structural arrangement to accommodate the multiple subsystems within a 16U CubeSat structure.

Future work includes carrying out detailed mission analysis, a thorough thermal analysis to refine heater power and coatings, a refinement of link budgets, and performing a combined optimization of mission trajectory and thruster performance.

MARIO shall introduce a paradigm shift in solar system exploration by performing significant science at very low costs. Although the risk is higher than that of traditional interplanetary missions, the gain is significantly high.

References

[1] T. H. Zurbuchen, R. von Steiger, S. Bartalev, X. Dong, M. Falanga, R. Fléron, A. Gregorio, T. S. Horbury, D. Klumpar, M. Küppers, *et al.*, "Perform-

ing high-quality science on cubesats," *Space Research Today*, vol. 196, pp. 11–30, Jan 2016.

[2] F. Topputo, M. Massari, J. Biggs, P. Di Lizia, D. Dei Tos, K. Mani, S. Ceccherini, V. Franzese, A. Cervone, P. Sundaramoorthy, *et al.*, "Lumio: Charazterizing lunar meteoroid impacts with a cubesat," in *69th International Astronaut. Congr. (IAC 2018)*, pp. 1–11, 2018.

[3] R. Staehle, D. Blaney, H. Hemmati, M. Lo, P. Mouroulis, P. Pingree, T. Wilson, J. Puig-Suari, A. Williams, B. Betts, *et al.*, "Interplanetary cubesats: opening the solar system to a broad community at lower cost," *Journal of Small Satellites*, vol. 2, no. 1, pp. 161–186, 2013.

[4] J. A. Wood, W. V. Boynton, W. R. Buck, J. P. Ferris, J. M. Hayes, K. J. Meech, J. F. Mustard, A. F. Nagy, K. S. Noll, D. A. Paige, R. T. Pappalardo, A.-L. Reysenbach, J. W. Schopf, and A. L. Sprague, *Assessment of Mars science and mission priorities*. Washington D.C: Space Studies Board, National Research Council, National Academies Press, 2003. ISBN: 978-0309089173.

[5] A. Klesh, B. Clement, C. Colley, J. Essmiller, D. Forgette, J. Krajewski, A. Marinan, T. Martin-Mur, J. Steinkraus, D. Sternberg, *et al.*, "MarCO: Early Operations of the First CubeSats to Mars," in *32nd Annual AIAA/USU Conference on Small Satellites, Logan, Utah, United States*, pp. 1–10, Aug 2018.

[6] R. Walker, D. Binns, C. Bramanti, M. Casasco, P. Concari, D. Izzo, D. Feili, P. Fernandez, J. G. Fernandez, P. Hager, *et al.*, "Deep-space cubesats: thinking inside the box," *Astronomy and Geophysics*, vol. 59, no. 5, pp. 5–24, 2018.

[7] F. Topputo and E. Belbruno, "Earth–Mars transfers with ballistic capture," *Celestial Mechanics and Dynamical Astronomy*, vol. 121, no. 4, pp. 329–346, 2015.

[8] K. V. Mani, A. Cervone, and F. Topputo, "Combined chemical–electric propulsion for a stand-alone mars cubesat," *Journal of Spacecraft and Rockets*, pp. 1–15, 2019.

[9] C. Scharlemann and M. Tajmar, "Development of propulsion means for microsatellites," in *43rd AIAA - American Society of Mechanical Engineers - Society of Automotive Engineers - American Society for Engineering Education Joint Propulsion Conference & Exhibit*, p. 5184, July 2007.

[10] K. Anflo and B. Crowe, "In-space demonstration of an ADN-based propulsion system," in *47th AIAA - American Society of Mechanical Engineers - Society of Automotive Engineers - American Society for Engineering Education Joint Propulsion Conference & Exhibit*, p. 5832, July 2011.

[11] A. S. Gohardani, J. Stanojev, A. Demairé, K. Anflo, M. Persson, N. Wingborg, and C. Nilsson, "Green space propulsion: Opportunities and prospects," *Progress in Aerospace Sciences*, vol. 71, pp. 128–149, Nov 2014.

[12] M. Negri, "Replacement of hydrazine: overview and first results of the h2020 project rheform," in *6th European Conference for Aeronautics and Space Sciences (EUCASS)*, pp. 29–06, June 2015.

[13] G. P. Sutton and O. Biblarz, *Rocket propulsion elements*, ch. 3, 9, pp. 55–68 & 90–92 & 282–284 & 342. John Wiley & Sons, 7 ed., 2010. ISBN: 978-0471326427.

[14] J. R. Wertz, D. F. Everett, and J. J. Puschell, *Space mission engineering: the new SMAD*, ch. 18, pp. 545–546. Microcosm Press, 2011. ISBN: 978-1881883159.

[15] G. Welsch, R. Boyer, and E. Collings, *Materials properties handbook: titanium alloys*. ASM international, 1993. ISBN: 978-0871704818.

[16] D. K. Huzel, *Modern engineering for design of liquid-propellant rocket engines*, vol. 147, ch. 8, pp. 289–304. AIAA, 1992. ISBN: 978-1563470134.

[17] M. Tsay, J. Frongillo, and J. Zwahlen, "Maturation of iodine fueled BIT-3 RF ion thruster and RF neutralizer," in *52nd AIAA - Society of Automotive Engineers - American Society for Engineering Education Joint Propulsion Conference*, p. 4544, July 2016.

[18] J. A. Gutierrez Ahumada, "Targeting a mars science orbit from earth using dual chemical-electric propulsion and ballistic capture," Master's thesis, Delft University of Technology, 2019.

[19] R. E. Hodges, N. Chahat, D. J. Hoppe, and J. D. Vacchione, "A deployable high-gain antenna bound for mars: Developing a new folded-panel reflectarray for the first cubesat mission to mars.," *IEEE Antennas and Propagation Magazine*, vol. 59, no. 2, pp. 39–49, 2017.

[20] W. J. Larson and J. R. Wertz, "Space mission analysis and design," tech. rep., Torrance, CA (United States); Microcosm, Inc., 1992.

[21] V. Franzese, P. Di Lizia, and F. Topputo, "Autonomous optical navigation for the lunar meteoroid impacts observer," *Journal of Guidance, Control, and Dynamics*, vol. 42, no. 7, pp. 1579–1586, 2019. DOI: 10.2514/1.G003999.

[22] V. Franzese, K. V. Mani, and F. Topputo, "Autonomous optical navigation for interplanetary cubesats," *24th AIDAA*, pp. 1–8, 2017.